ふ　なんなん
氏　　名　胡　南南
授　与　学　位　博士（工学）
学位授与年月日　平成２４年３月２７日
学位授与の根拠法規　学位規則第４条第１項
研究科，専攻の名称　東北大学大学院工学研究科（博士課程）電気・通信工学専攻
学位論文題目　Study on Superconducting Property of Tri-axial High Temperature Superconducting Power Cable（三相同軸型高温超電導ケーブルの超電導特性に関する研究）
指導教員　東北大学教授　濱島　高太郎
論文審査委員　主査　東北大学教授　濱島　高太郎　東北大学教授　一ノ倉　理
東北大学教授　安藤　晃　東北大学准教授　津田　真

論文内容要旨

1. INTRODUCTION

Tri-axial HTS cable has been intensively investigated and recently connected to the commercial power network in practice project.[1-3] However, because the HTS tri-axial cable is composed of three concentric layers with different radius, there is an inherent unbalanced current distribution in the tri-axial cable. Also in practical application, before the cable can be installed in the grid, it has to show reliable performance during any fault conditions. After the quench, cable is removed from the power network by a breaker. A recovery time is also a very important parameter to decide if the cable is allowed to be reconnected to the power network.

In this paper, first, we will propose an improved cable twist pitch design to solve the imbalance problem in existent tri-axial cable. Second, we will develop an AC loss calculation method in out-of-phase magnetic fields for tri-axial cable. Third, we will evaluate the tri-axial cable thermal stability by developing a computational heat transfer code to simulate transient thermal behaviors after the fault.

2. THEORY OF BALANCED TRI_AXIAL CABLE

As shown in Fig. 1, we proposed a tri-axial cable composed of two longitudinal sections with different twist pitches. In this calculation we assume that, compared with cross-section, the length of the cable is long enough to ignore the interaction between sections.

In superconducting condition, voltage drop of the cable mainly comes from inductance. Then the voltage drop of phase k is described as following equation:

$$\dot{V}_k = j\omega \times \sum_{i=a}^{c} \sum_{s=1}^{2} l_s \times M_{k,i,s} \times \dot{I}_i \tag{1}$$

where

$$\begin{aligned} M_{k,k,s} &= L_{k,s} = \frac{\mu_0}{2\pi} \ln \frac{1}{r_k} + \sum_{j=1}^{2} \frac{1}{2} \mu_0 \pi r_k^2 \left(\frac{1}{p_{k,j}} \right)^2 \\ M_{k,i,s} &= M_{i,k,s} = \frac{\mu_0}{2\pi} \ln \frac{1}{r_k} + \sum_{j=1}^{2} \frac{1}{2} \mu_0 \pi r_i^2 \left(\frac{1}{p_{k,j}} \right) \left(\frac{1}{p_{i,j}} \right) \\ & \qquad for \left(r_k > r_i \right) \end{aligned} \tag{2}$$

here ω is angular frequency. l_s is the cable length of each section in longitudinal direction. p_{kj} is the twist pitch of phase k, p_{ij} is the twist pitch of phase i; r_k is radius of phase k; μ_0 is the permeability of the free space; $L_{k,s}$ is self-inductance of phase k, $M_{k,i,s}$ is mutual-inductance between phase k and phase i.

We also have the symmetrical condition that present as following equations:

$$\begin{aligned} V_b &= \alpha^2 V_a, V_c = \alpha V_a \\ I_b &= \alpha^2 I_a, I_c = \alpha I_a \end{aligned} \tag{3}$$

here, a phase rotation operator α is defined to rotate a phase vector forward by 120 degrees. Inserting equation (1) into symmetrical condition equation (3), we get the general equations, satisfying the balanced three-phase currents restrict, is a function of radius and twist pitch. That means that balance current distribution could be realized by reasonable twist pitches design.

Based on this theory, we designed and fabricated a prototype HTS tri-axial cable. [3] The test result which is shown in Fig. 3 demonstrates that the theory is right for an equivalent impedance circuit model.

3. AC LOSS

Since the cable has a concentric configuration, the magnetic field on both surface of the current layer has an out-of-phase problem due to out-of-phase transport currents in next layers. An alternated AC loss calculation method is needed for tri-axial cable loss evaluation.

Because external field parallel apply to the tape's wide surface, we can use a Bean slab model to analyze the AC loss. For out-of-phase magnetic field condition, equations (4), (5), and (6) will be used for AC loss calculation.

$$b_m = B_m / B_p, \quad b'_m = B'_m / B_p, \quad B_p = \mu_0 J_c d \tag{4}$$

$$Q_1 = \frac{B_p^2}{3\mu_0}(b_m^3 + b_m'^3) \text{ [J/m}^3\text{/cycle]} \quad (b_m + b'_m < 2) \tag{5}$$

$$\begin{aligned} Q_2 = {} & \frac{B_p^2}{24\mu_0}[b_m^3(5-3\cos 2\omega t_1) + b_m'^3\{5-3\cos 2(\omega t_1 - \phi_0)\} \\ & + b_m^2 b'_m\{-4\cos\phi_0 + 3\sin(\omega t_1 + \phi_0) - \sin(3\omega t_1 - \phi_0)\} \\ & + b_m b_m'^2\{-3-\cos 2\phi_0 + 3\sin(\omega t_1 - 2\phi_0) - \sin(3\omega t_1 - 2\phi_0)\} \\ & + b_m^2(6+6\cos 2\omega t_1) + b_m'^2\{6+6\cos 2(\omega t_1 - \phi_0)\}] \quad (b_m + b'_m > 2) \end{aligned} \tag{6}$$

where B_p is the penetration field, b_m, b'_m are the normalized field on the inner and outer surface. Q_1 is the AC loss expression when the applied field less than tape penetration field. Q_2 is the AC loss when the applied field larger than tape penetration field. And t_1, when the inner or outer field suddenly changed, is defined as the shorter time of following equations:

$$\sin(\omega t_1 - \phi_0) = \frac{2 - b_m}{b'_m}, \quad \sin\omega t_1 = \frac{2 - b'_m}{b_m} \tag{7}$$

Then the AC loss is converted from per cubic meter volume to per meter length by using following equation.

$$Q' = Q \cdot f \cdot n \cdot t \cdot \frac{w}{\cos\theta} \text{ [W/m]}, \quad \theta = \text{ArcTan}\left(\frac{2\pi r}{p}\right) \tag{8}$$

By using above equations, an AC loss calculation comparison between 1layer/phase tri-axial and triad-coaxial cable is carried out to

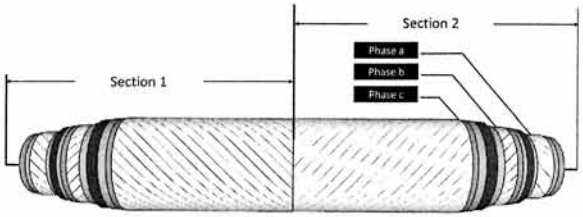

Fig. 1 Two-section tri-axial HTS cable.

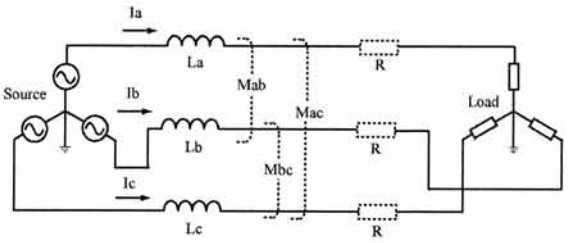

Fig. 2 Equivalent circuit.

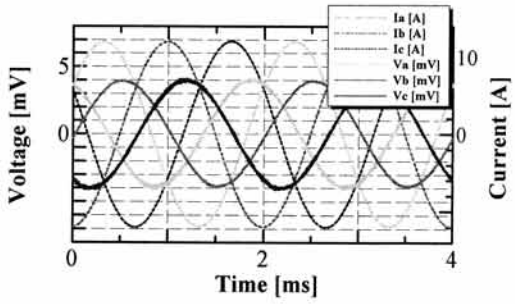

Fig. 3 Verification test result.

Table 1 Cable parameter.

Nominal power (MVA)	350
Nominal voltage (kV)	66
Nominal current (kA)	3
Outer diameter (mm)	130
130mm 1layer/phase triad-coaxial cable	
Critical current(kA)	5
Twist pitch of conductor and shield p_{co},p_s(mm)	p_{co}: parameter p_s: parameter
130mm 1layer/phase tri-axial cable	
Critical current(kA)	7.2
Twist pitch (mm)	$p_{c1}=p_{c2}$, p_{a1} : parameter

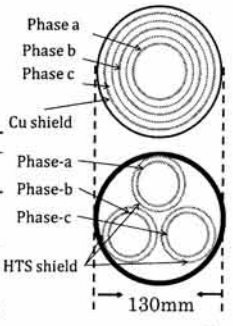

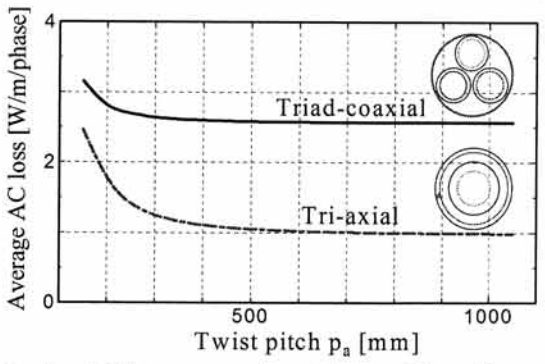

Fig. 4 AC loss comparison between 1layer/phase tri-axial and triad-coaxial cable.

investigate if tri-axial structure have an advantage over triad-coaxial structure in loss. The result is shown in Fig. 4. The calculation shows that loss decrease with the increasing twist pitch; The AC loss in tri-axial model is lower than the aim value of NEDO which have 1 W/m/phase AC loss. In same size, voltage class, and power capacity; AC Loss of tri-axial cable less than triad-coaxial cable. [4-5]

4. OVER CURRENT & RECOVERY ANALYSIS

In the cable safety design, one principle for the design is that cable should survive in a worst fault. The maximum fault current used in this calculation is referenced Japanese electro technical committee (JEC) current test stand which gives a 31.5kA fault current with 2 seconds duration time for 66kV distribution power system. Since each cable phase consist of a current HTS layer and a stabilizer copper layer, the maximum temperature rise of the cable could be controlled by the stabilizer thickness. Therefore a safety cable design will be carried out in the worst fault and cooling case. A reasonable thickness of stabilizer layer design will be proposed to guarantee the cable safety in maximum temperature rise. Here, phase b is sandwiched by insulation a layer which has the worst cooling environment is marked as the target.

Moreover, after the quenched cable is removed from the power network by a breaker, a recovery time is also a very important parameter to decide if the cable is allowed to be reconnected to the power network. In the tri-axial structure, three phases may have different recovery times due to an unsymmetrical cooling configuration. Low thermal conductivity of OPPL insulation layer may cause long recovery times for phase-b and phase-c. Therefore, we developed a code, and accomplished a simulation including the consideration of thermal conductivity of each cable layer.

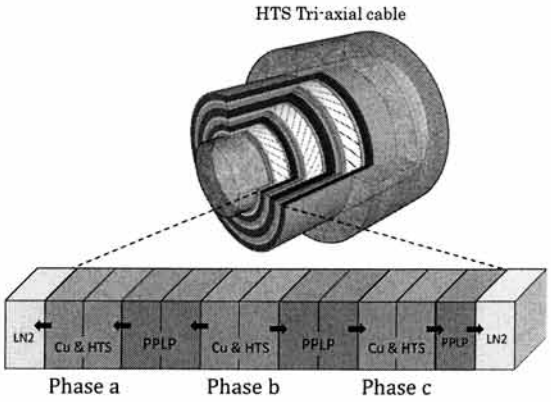

Fig. 5 Unsymmetrical cooling configuration of tri-axial cable.

Table 2 Cable parameter for calculation.

Insulation thickness	5.5mm,5.5mm,3mm
Inner diameter	87mm
Outer diameter	130mm
Area of Cu stabilizer	500mm^2
Inlet Liquid nitrogen temperature	70K (constant)
Radius Mesh size	0.0005mm
Heat capacity of OPPL*	0.8×10^6 J/m^3.k
Thermal conductivity of OPPL	0.1w/m · K
Mesh number	140

The heat balance equation is used to simulate the cable temperature T_M along the radial direction:

$$\rho c\frac{\partial T_M}{\partial t}=\frac{1}{r}\frac{\partial}{\partial r}\left(kr\frac{\partial T_M}{\partial r}\right)+G(T_M,i) \tag{9}$$

here ρ, c, k is the density, specific heat and thermal conductivity of each layer, respectively.

The calculation parameters are listed in Table 2. Equation (9) is solved by using Crank Nicolson implicit method.

The cable boundary condition in worst condition is assumed as adiabatic heat generation state in fault. Heat transfer part in the equation becomes to be zero. Heat generation in the fault based on the voltage drop analysis is calculated by:

$$\begin{aligned} &T_M \le T_c \\ &G(T_M,i)=\begin{cases} 0 & i\le I_c(T_M) \\ \lambda_{av}(T_M)\dfrac{1}{S^2}i\left(i-I_c(T_M)\right) & i\ge I_c(T_M) \end{cases} \\ &T_M \ge T_c \\ &G(T_M,i)=\lambda_{av}(T_M)\left(\frac{i}{S}\right)^2 \end{aligned} \tag{10}$$

where T_c is the critical temperature of the current layer, λ_{av} is the average resistivity of the Cu stabilizer and Ag sheath.

The heat transfer coefficient h at both surfaces is given by Dittus-Boelter equation:

$$h=0.023\cdot \mathrm{Re}^{0.8}\cdot \mathrm{Pr}^{0.4}\cdot\frac{k_F}{D_{in}} \tag{11}$$

where D_{in} is the inside hydraulic diameter. k_F, Re, Pr are temperature dependent thermal conductivity, Reynolds number and Prandtl

number of LN_2, respectively.

2.2. Numerical computation results

In over current analysis, the thickness of stabilizer is varied from 0.6 mm to 2.8 mm. The maximum temperature of phase-b as a function of thickness of copper stabilizer is shown in Fig. 6. The figure indicates that the temperatures decrease with the increasing copper thickness. Copper stabilizer design should keep phase-b' temperature in safety range in the worst fault condition.

In recovery analysis, Fig. 7 shows a simulation result of a temperature profile when the SLG fault occurs in phase-b. Fig. 7(a) shows the temperature profile from 0 to 100 seconds. In our design, the maximum temperature rise in the worst condition Fig. 7(b) shows the temperature profile from 100 to 1000 seconds. Fig. 7 shows that even after 1000s, temperature of phase-b still haven't return to initial value due to low thermal conductivity of insulation layer. It means that the thickness of OPPL is one of the key elements for recovery time and a thinner insulation layer will lead to a fast recovery. [6-7]

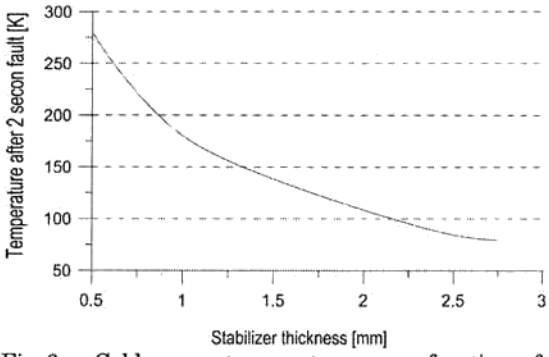

Fig. 6 Cable max temperature as a function of copper stabilizer thickness.

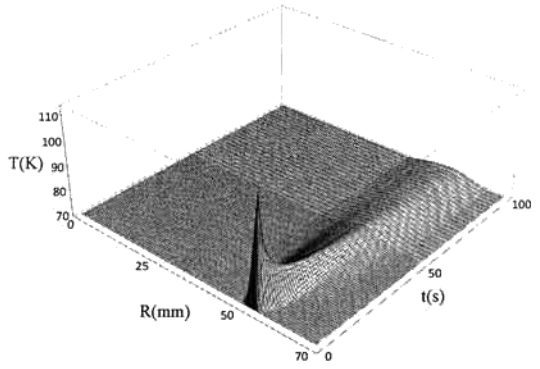

(a) 0-100s

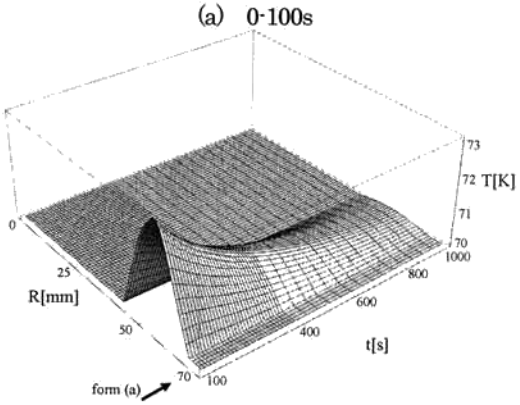

(b) 100-1000s

Fig. 7 Temperature profile in radial direction

5. SUMMARY

This research has devised a guide for design and evaluation of a balanced tri-axial cable. The reasonable twist pitch design could realize a balanced current distribution. Based on our design, the thermal stability evaluation demonstrates the reliability in practical use. The research results indicate the utility and possibility of the application of improved tri-axial HTS cable.

REFERENCE

1) J.A.Demko, I.Sauers, D.R.James, M.J.Gouge, D.Lindsay, M.Roden, J.Tolbert, D.Willen, C.T.Neilsen and C.Traeholt, "Tri-axial HTS Cable for the AEP Bixby Project", IEEE Trans. Appl. Supercond. No.17, 2007, pp.2047-2050
2) T. Masuda, H. Yumura, and M. Watanabe, "Recent Progress of HTS Cable Project", Physica C 468, 2008, pp.2014–2017
3) T. Hamajima, T. Yagai, and M. Tsuda, "Analysis of Balanced Three-Phase Current Distributions in a Tri-Axial Cable", IEEE Trans. Appl. Supercond., No.16, 2006, pp.1586-1589
4) Hamajima. T, Tsuda. M, Yagai. T, S. Monma, H. Satoh, and K. Shimoyama 2007 Analysis of AC Losses in a Tri-axial Superconducting Cable IEEE Trans. Appl. Supercond. 17 1692-1695.
5) N. Hu, M. Toda, O. Nuri, T. Yagai, M. Tsuda, and T. Hamajima, "Optimization of AC Losses in Tri-axial HTS Cable with Balanced Three-phase Current Distribution", EUCAS 2009, No.158, 2009
6) N. Hu, M. Toda, A. N. Ozcivan, T. Yagai, M. Tsuda, and T. Hamajima, "Fault Current Analysis in a Tri-axial HTS Cable", IEEE Trans. Appl. Supercond., Vol.20, No.3 2010, pp.1288-1291
7) N. HU, M. Toda, T. Watanabe, M. Tsuda, and T. Hamajima "Recovery Time Analysis in a Tri-axial HTS Cable after an Over-current Fault", Physica C 471 (2011) 1295–1299

論文審査結果の要旨

高温超電導体を用いた超電導ケーブルは，従来の電力ケーブルと比べて低損失かつコンパクトになることから，CO_2削減・省エネルギー・省スペースなどの面で大いに期待されている。特に，三相同軸型高温超電導ケーブルは三相平衡状態で漏洩磁界が発生しない特性を有するためコンパクトで経済性のある構成となるが，同軸構造のために生じる三相不平衡の改善が電力ケーブルを実現する上で重要な課題となっている。本論文は，三相同軸型高温超電導ケーブルの実用化を目的として，三相同軸ケーブルの平衡電流分布構成の提案，およびその実験的検証，ケーブルの交流損失の最小化，絶縁設計，送電特性，および事故時の熱設計指針に関する研究をまとめたもので，全編７章からなる。

第１章は緒言であり，本研究の背景と目的を述べている。

第２章では，超電導線材を用いた三相同軸型超電導ケーブルで三相平衡電流分布を得るための新しい構成理論の提案と，その実証試験結果を述べている。三相同軸ケーブルは種々のケーブル構造の中で超電導線材の量が最も少なくコンパクトにできる構造であるが，等しいピッチで線材を巻きつけた構成では，各相の電流分布が不平衡状態となり，不平衡電流成分が中性線に流れて大きな損失や電圧の不均一をひきおこす。本論文では，ケーブルを２分割して線材の巻ピッチを調整することにより理論的に三相平衡電流分布が実現できることを初めて提案し，長さ１ mの超電導ケーブルを設計製作して実証した。これは三相同軸超電導ケーブルを実用化する上で極めて有用な成果である。

第３章では，三相同軸超電導ケーブルの交流損失を最小化する構成を明確にしている。通電電流と外部磁界の位相が異なる場合の新しい交流損失解析方法を提案して，交流損失を最小化できる超電導線のピッチ構成を考案した。これは三相同軸超電導ケーブルの交流損失を低減する上で重要な成果である。

第４章では，三相同軸ケーブルの絶縁物を極低温下の限られた空間内に構成するために，事故時に絶縁破壊しない絶縁材料と厚さの関係を明らかにしている。三相平衡電流分布状態にあるケーブルの各相半径と電界の関係式を求めて必要な電気絶縁層厚さを明確に示した。これは三相同軸ケーブルの絶縁設計に有用な成果である。

第５章では，三相同軸ケーブルを配電系統に設置した時に，ケーブルの各相間の静電容量や製作誤差などが輸送特性に与える影響について検討を行い，ケーブルの長さに伴って不平衡状態は徐々に大きくなるが，配電系統に適用する数 km程度のケーブル長では不平衡率が小さいことを明らかにした。この成果は実際のケーブルを設置する場合に有効である。

第６章では，平衡状態にある三相同軸ケーブルの事故時の非定常熱解析を行い，ケーブルが焼損しない安定化銅の厚みなどを明らかにしている。熱解析では，超電導ケーブルの熱伝導方程式と，冷媒である液体窒素の非定常流体方程式に基づいて事故時の超電導ケーブルの過渡特性のシミュレーションを行っている。その結果，最も厳しい規格試験条件を満たす安定化銅の厚みは約２ mmであること，超電導状態への復帰時間は低い熱伝導率を持つ絶縁層の厚みに大きく依存することを明確にした。これらは三相同軸ケーブルの熱設計指針として実用上高く評価される。

第７章は結言である。

以上要するに本論文は，高温超電導線を用いた三相同軸ケーブルを実現するために，三相平衡電流分布の構成理論の提案とその実証，また，実用化のための絶縁設計，事故時の非定常熱解析技術を確立したもので，電気工学および超電導応用分野の発展に寄与するところが少なくない。

よって、本論文は博士(工学)の学位論文として合格と認める。